

Optical-resolution photoacoustic microscopy for *in vivo* imaging of single capillaries

Konstantin Maslov,¹ Hao F. Zhang,^{1,2} Song Hu,¹ and Lihong V. Wang^{1,*}

¹Department of Biomedical Engineering, Optical Imaging Laboratory, Washington University in St. Louis, Campus Box 1097, One Brookings Drive, St. Louis, Missouri 63130-4899, USA

²Current address: Department of Electrical Engineering and Computer Science, University of Wisconsin-Milwaukee, P.O. Box 748, Milwaukee, Wisconsin 53201-0784, USA

*Corresponding author: lhwang@biomed.wustl.edu

Received January 30, 2008; accepted March 2, 2008;
posted March 20, 2008 (Doc. ID 92316); published April 23, 2008

Capillaries, the smallest blood vessels, are the distal end of the vasculature where oxygen and nutrients are exchanged between blood and tissue. Hence, noninvasive imaging of capillaries and function *in vivo* has long been desired as a window to studying fundamental physiology, such as neurovascular coupling. Existing imaging modalities cannot provide the required sensitivity and spatial resolution. We present *in vivo* imaging of the microvasculature including single capillaries in mice using optical-resolution photoacoustic microscopy (OR-PAM) developed in our laboratory. OR-PAM provides a lateral resolution of 5 μm and an imaging depth >0.7 mm. © 2008 Optical Society of America
OCIS codes: 170.3880, 170.5120, 180.5810.

The advantages of photoacoustic microscopy (PAM) over traditional optical and ultrasonic imaging primarily include the detection of endogenous optical absorption contrast at ultrasonic resolutions [1,2]. In PAM, a pulsed laser beam is weakly focused into the biological tissue to produce emission of ultrasonic waves owing to thermal expansion of the medium caused by absorbed laser radiation. The ultrasonic waves are then detected with a focused ultrasonic transducer to form high-resolution volumetric images. Among the existing photoacoustic imaging technologies, the spatial resolutions almost solely depend on the ultrasonic parameters including the frequency and the numerical aperture (NA). For example, in the recently developed dark-field confocal PAM, a lateral resolution of 50 μm was achieved with a center frequency of 50 MHz and an NA of 0.44 [3]. This resolution is adequate for many biomedical applications [2,4]. However, to resolve smaller structures, such as capillaries that are 4–9 μm in diameter [5], higher spatial resolution is required.

If both the lateral and axial resolutions are ultrasonically provided, the imaging penetration is limited by the frequency-dependent ultrasonic attenuation in tissue. For example, a 5 μm lateral resolution requires an ultrasonic center frequency >300 MHz. At such a high frequency, the ultrasonic attenuation (~ 20 dB/mm in water and ~ 80 dB/mm in tissue) limits the penetration depth to ~ 100 μm , which is less than that of optical confocal microscopy. An alternative is to use fine optical focusing to provide the lateral resolution while the axial resolution is still derived from time-resolved ultrasonic detection. We refer to this alternative technology as optical-resolution photoacoustic microscopy (OR-PAM). Although having a comparable depth penetration limit with existing high-resolution optical imaging modalities (including optical confocal microscopy, two-photon microscopy, and optical coherence tomography), OR-PAM is primarily sensitive to optical

absorption contrast, whereas the other modalities are dominantly sensitive to optical scattering or fluorescence contrast.

Our OR-PAM system (Fig. 1) employs optical focusing to achieve micrometer-level lateral resolution. A dye laser pumped by an Nd:YLF laser is used as the irradiation source. Laser pulses (pulse duration, 7 ns) from the dye laser are spatially filtered by a 25 μm diameter pinhole. The pinhole is then imaged to a diffraction-limited focal spot with a diameter of 3.7 μm by an objective lens (NA, 0.1; depth of focus, ~ 40 μm). The laser pulse energy after the objective lens is measured to be 100 nJ. Ultrasonic focusing is achieved through a plano-concave lens (radius of curvature, 5.2 mm; aperture, 6.4 mm; NA in water, 0.46). The optical objective lens and 75 MHz ultrasonic transducer (V2022 BC, Olympus NDT) are coaxially and confocally configured as shown in Fig. 1.

A combination of time-resolved detection of the photoacoustic waves with a two-dimensional (2D) raster scanning along the x - y plane generates a volumetric image [4], which can be viewed through direct volumetric rendering, cross sectional (*B*-scan) images, or maximum amplitude projection (MAP) images [4].

The imaging depth of the OR-PAM system was measured by imaging two horse hairs (diameter,

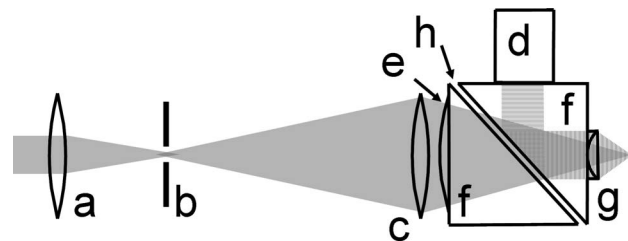


Fig. 1. Schematic of the OR-PAM system. a, Condenser lens; b, pinhole; c, microscope objective; d, ultrasonic transducer; e, correcting lens; f, isosceles prism; g, acoustic lens; h, silicon oil.

200 μm) separately placed above and below a piece of freshly harvested rat scalp. An OR-PAM image (Fig. 2A) was acquired with 32 times signal averaging at the optical wavelength of 630 nm. Both hairs are clearly visible. The B-scan image (Fig. 2B) shows that the bottom hair is 700 μm deep in the tissue. Therefore, the imaging penetration limit is at least 700 μm .

The axial resolution was estimated to be 15 μm based on the measured transducer bandwidth (100 MHz in receiving-only mode) and the speed of sound in tissue (1.5 mm/ μs). The lateral resolution of the OR-PAM system in an optically clear medium was experimentally measured by imaging a United States Air Force (USAF-1951, Edmund) resolution test target. Images were acquired at the optical wavelength of 590 nm. In Fig. 2C, the highlighted well-resolved bars (group 6, element 5) have gaps of 4.9 μm (spatial frequency, 102 mm^{-1} ; modulation transfer function value, 0.65). Other pairs of spatial frequency and modulation transfer function values are 64 mm^{-1} with 0.95 and 80 mm^{-1} with 0.8. Non-linearly fitting the modulation transfer function followed by extrapolation yields a lateral resolution of 5 μm , which is 30% greater than the diffraction limit of 3.7 μm . To further illustrate of the lateral resolution, a MAP image of a 6 μm diameter carbon fiber immersed in water is shown in Fig. 2D. The mean full width at half-maximum (FWHM) value of the imaged fiber is estimated to be 9.8 μm , which is 3.8 μm wider than the fiber diameter and hence in agreement with the 5 μm resolution. Since the lateral resolution is expected to deteriorate with an imaging depth owing to optical scattering, a 6 μm diameter carbon fiber covered by a 0.2 mm thick nude mouse ear was imaged. The photoacoustic amplitude profile of a cross section of this carbon fiber is shown in Fig. 2E. The FWHM value of the imaged fiber is estimated to be 10 μm . Hence OR-PAM maintains an ~ 5 μm lateral resolution in tissue up to at least 0.2 mm in depth.

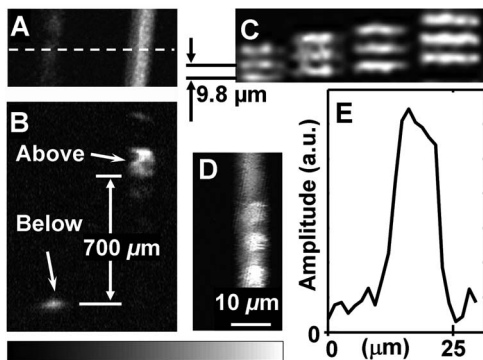


Fig. 2. Imaging depth and lateral resolution of the OR-PAM system. A, MAP image of two horse hairs placed above and below a piece of rat skin; B, B-scan image at the location marked by the dashed line in A; C, MAP image of a USAF resolution test target group 6; D, MAP image of a 6 μm diameter carbon fiber; E, Cross-sectional profile of a 6 μm diameter carbon fiber under a 0.2 mm thick nude mouse ear.

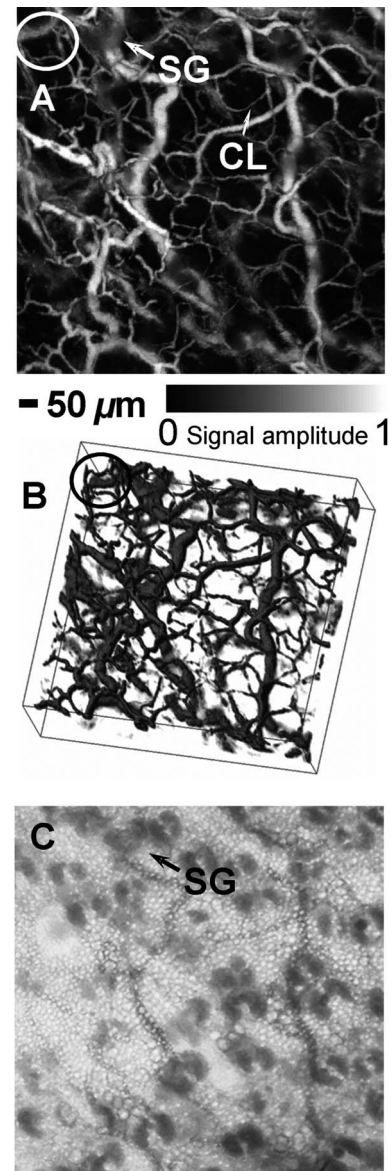


Fig. 3. Microvasculature in a nude mouse ear. A, *In vivo* OR-PAM image; B, 3D pseudocolor visualization of the vasculature; C, photograph taken with transmission optical microscopy; CL, capillary, and SG, sebaceous gland.

The major optical absorbers in the visible spectral range in biological tissue include deoxyhemoglobin and oxyhemoglobin. Consequently, PAM, acting as a sensitive blood detector with high contrast and specificity, is suitable for imaging the volumetric morphology of subcutaneous microvasculature *in vivo*.

We applied the OR-PAM to image the microvasculature in the ear of a nude mouse (Hsd, Athymic Nude-Foxn1^{NU}, Harlan Co.; body weight, 20 g) *in vivo* at the optical wavelength of 578 nm. All experimental animal procedures were carried out in conformity with the laboratory animal protocol approved by the School of Medicine Animal Studies Committee of Washington University in St. Louis. Nude mouse ears (thickness, ~ 300 μm) have well-developed vasculature and have been widely used to study tumor angiogenesis and other microvascular diseases [6,7]. During image acquisition, the animal, warmed by an

infrared lamp, was kept motionless using a breathing anesthesia system (E-Z Anesthesia, Euthanex). Unlike that in [8], no optical clearing agent was applied to the skin surface. An area of $1\text{ mm} \times 1\text{ mm}$ was scanned with a step size of $1.25\text{ }\mu\text{m}$ without signal averaging. The scanning time for a complete volumetric dataset was ~ 10 min. After data acquisition, the animal naturally recovered without observable laser damage.

The OR-PAM images of the microvasculature (Figs. 3A and 3B) agree with the photograph (Fig. 3C) taken with a transmission optical microscope at a $4\times$ magnification; however, small vessels are observed only in the OR-PAM images. The mean ratio of the photoacoustic amplitudes between the blood vessels and the background is 20:1, which demonstrates a high endogenous optical-absorption-based contrast. Some vessels, such as the vessel labeled with CL in Fig. 3, have diameters of $\sim 5\text{ }\mu\text{m}$ and hence are most probably single capillaries. A volumetric rendering of the photoacoustic data (Fig. 3B) shows the three-dimensional (3D) spatial positions and connectivity of the blood vessels. For example, at the center of the circle in Fig. 3B, the small-diameter vessel invisible in the MAP image in Fig. 3A is clearly seen $\sim 100\text{ }\mu\text{m}$ above the larger vessel. In addition, vessel branching is clearly observed. Therefore, OR-PAM is able to image single capillaries *in vivo* with endogenous contrast owing to the optical absorption of hemoglobin.

The capability of OR-PAM to image physiological and pathological changes in capillaries and other microvessels has potentially broad applications. Possible applications include microscopic imaging of vasodilation and vasoconstriction in stroke, tumor angiogenesis, tumor extravasations, and tumor metabolic rate of oxygen consumption. Mouse ears were chosen as the initial organ to test OR-PAM because in this case transmission optical microscopy can be used to validate some of our results. Since OR-PAM operates in the reflection mode, it can be applied to many other anatomical sites.

When the optical focus is $100\text{ }\mu\text{m}$ below the tissue surface, the surface optical fluence is close to the

American National Standards Institute (ANSI) safety limit (20 mJ/cm^2 in the visible spectral region) [9]. Although the ANSI standards regulate only the surface fluence, here we compute the spatial peak optical fluence at the focus in water, which is 500 mJ/cm^2 . This focal fluence is still less than the damage threshold experimentally observed in small animals [8]. By redesigning the acoustic coupling cube to transmit photoacoustic waves without transformation from *p*-waves into sv-waves and applying an acoustic antireflection coating on the lens, acoustic losses can be reduced by $\sim 24\text{ dB}$. Hence the optical fluence can be reduced to the ANSI safety limits without affecting the signal-to-noise ratio (SNR).

This research was sponsored in part by the National Institutes of Health grants R01 EB000712 and R01 NS46214 Bioengineering Research Partnership. The authors contributed equally to this work.

References

1. H. F. Zhang, K. Maslov, G. Stoica, and L. V. Wang, *Nat. Biotechnol.* **24**, 848 (2006).
2. A. A. Oraevsky and A. A. Karabutov, "Optoacoustic tomography," in *Biomedical Photonics Handbook*, T. Vo-Dinh, ed. (CRC Press, 2003), Vol. PM125, Chap. 34.
3. K. Maslov, G. Stoica, and L. V. Wang, *Opt. Lett.* **30**, 625 (2005).
4. H. F. Zhang, K. Maslov, and L. V. Wang, *Nat. Protocols* **4**, 797 (2007).
5. A. C. Guyton and J. E. Hall, *Textbook of Medical Physiology* (Saunders, 2000).
6. S. Basu, J. A. Nagy, S. Pal, E. Vasile, I. A. Eckelhoefer, V. S. Bliss, E. J. Manseau, P. S. Dasgupta, H. F. Dvovrak, and D. Mukhopadhyay, *Nat. Med.* **7**, 569 (2001).
7. D. A. Elson, G. Thurston, L. E. Huang, D. G. Ginzinger, D. M. McDonald, R. S. Johnson, and J. M. Arbeit, *Genes Dev.* **15**, 2520 (2001).
8. V. P. Zharov, E. I. Galanzha, E. V. Shashkov, N. G. Khlebtsov, and V. V. Tuchin, *Opt. Lett.* **31**, 3623 (2006).
9. Laser Institute of America, *American National Standard for Safe Use of Lasers ANSI Z136.1-2000* (American National Standards Institute, Inc., 2000).